P3.12

AEROSOL OPTICAL DEPTH RETRIEVALS FROM HIGH-RESOLUTION COMMERICIAL SATELLITE IMAGERY OVER AREAS OF HIGH SURFACE REFLECTANCE

Dominick A. Vincent*
Kurt E. Nielsen
Philip A. Durkee
Naval Postgraduate School, Monterey, California
Jianglong Zhang
Jeffery S. Reid
Naval Research Laboratory, Marine Meteorology Division, Monterey, California

1. INTRODUCTION

Atmospheric aerosol particles impact the Earth's energy budget through reflection and absorption of solar radiation (the aerosol direct effect) and modification of cloud properties (the aerosol indirect effect). The scattering of incoming solar radiation back to space results in a net decrease in heating at the Earth's surface. The absorption of solar energy alters the atmospheric heating rate, which influences atmospheric circulation. The indirect effect works to increase cloud albedo at solar wavelengths by providing additional cloud condensation nuclei that often produce more and smaller drops that subsequently result in brighter clouds. Again, this reduces heating of the atmosphere and at the Earth's surface. When compared to the global heating caused by anthropogenic greenhouse gases, cooling due to aerosols has the potential to offset greenhouse gas warming by approximately 25 to 50% (IPCC 2001, Twomey *et al.* 1984, Charlson *et al.* 1992, Kiehl and Briegleb 1993). The effects of aerosol particles, however, are much harder to characterize and quantify than those of greenhouse gases. Greenhouse gases have a relatively homogeneous distribution globally and a lifetime of up to 100 years or more (IPCC 2001, Prather 1996, Smith and Wigley 2000). Aerosol particles have heterogeneous spatial and temporal distributions with life spans on the order of days to weeks (IPCC 2001). Recent research efforts, especially in the fields of remote sensing and modeling, have focused on characterizing the climatic effects of sources and distributions of natural and anthropogenic aerosols.

Much effort has been focused on aerosol characterization using satellite observations due to the extensive area covered by satellites combined with temporal resolutions usually on the order of a day or better. Over water aerosol characterization efforts have been successful (Brown 1997, Durkee et al. 2000, Kuciauskas 2002, Martin 2004, Abdou et al. 2005, Kahn et al. 2005, Remer et al. 2005). Product development over land has proven much more difficult due to the complexity added by the variability of the land surface characteristics (Odell and Weinman 1975, Tanre *et al.* 1981, Kaufman and Joseph 1982, Kaufman and Fraser 1984, Kaufman and Sendra 1988, Tanre et al. 1988, Tanre and Legrand 1991, Remer et al. 2005). Current satellite techniques for characterizing aerosols over land are highly background-dependent and require stable, dark bodies of water or vegetation. Many anthropogenic and terriginous aerosols derive from areas where such limitations cannot be accommodated (e.g., desert, coastal, or urban regions). Likewise, techniques such as DEEP BLUE as introduced in Hsu et al. (2004) can accommodate highly reflective backgrounds, but require multiple channels in the blue region of the visible spectrum that are only found on a limited number of sensors. For this reason, investigation of alternative methods for characterizing aerosol particles over land using satellite observations must continue.

The advancement and proliferation of commercial high-spatial resolution imaging satellites presents a new opportunity for overland aerosol characterization. Other methods employing high-spatial resolution satellite imagery have been developed for aerosol optical depth retrievals to include extension of the dark object method and contrast reduction methods (Kaufman and Sendra 1988, Tanre and Legrand 1991). Many of these efforts have met with difficulty due to surface characterization issues. With increased spatial resolution, enhanced surface complexity introduces further variability and uncertainty into aerosol optical depth estimations. The QuickBird satellite has a maximum spatial resolution of 2.44 meters for multi-spectral imagery and 0.61 meters

* *Corresponding author address:* Dominick A. Vincent, Naval Postgraduate School, 589 Dyer Rd., Rm 254, Monterey, CA 93943; e-mail: davincen@nps.edu.

for panchromatic imagery (DigitalGlobe 2005). This introduces a level of surface complexity not previously seen in environmental applications satellites. However, high-spatial resolution presents an opportunity to resolve individual image features, such as shadows, that contain aerosol information. Fig. 1 shows typical features found in QuickBird panchromatic imagery that may be used for AOD retrievals.

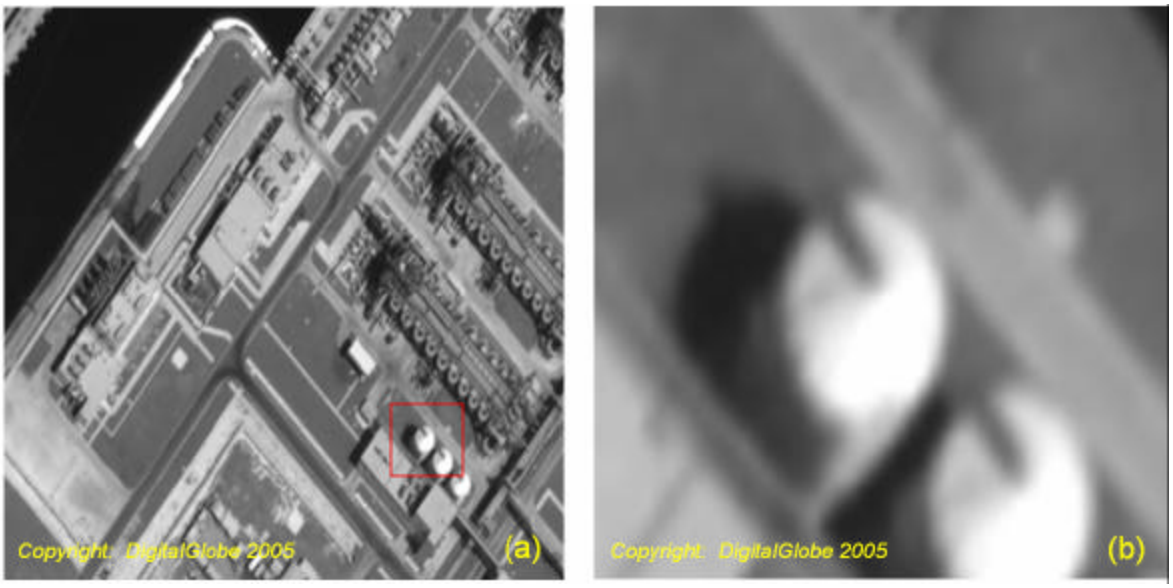

Figure 1. An example subset of a QuickBird panchromatic image of a water desalinization plant northwest of Abu Dhabi taken 26 September 2004: (a) general overview of the area and (b) a zoom showing and individual shadowed area (courtesy of DigitalGlobe).

2. SHADOW TECHNIQUE THEORY

A principles-of-invariance method of radiative transfer (hence forth POI) was chosen for this study rather than deriving the radiation field directly from the radiative transfer equation due to the POI's ability to partition the radiative effects more intuitively. The POI method is based on physical statements and mathematical formulations of the reflection and transmission of light as proposed by Ambartzumian (1958) and developed by Liou (2002). This is useful when comparing the resulting radiance fields for shaded and unshaded regions in high-spatial resolution imagery and allows one to selectively omit source terms where appropriate. The following development is based on the POI method of radiative transfer, including surface reflection, as presented by Liou (2002).

Separate photon budgets can be developed from Liou (2002) for the specific case of comparing the observed radiance found within and outside of shadow regions of high-spatial resolution imagery. By taking the difference between shaded and unshaded photon budgets, one is left with the difference in observed radiance as a function of target reflectance, mean aerosol reflectance, solar and sensor zenith angles, solar irradiance, and total optical depth. Total optical depth retrievals are possible if the remaining parameters are measured or known. The resulting total optical depth can be partitioned into effects from ozone, water vapor, molecular Rayleigh scattering and aerosol effects. Since current commercial high-spatial resolution imagery only covers the visible and near-infrared portions of the spectrum and is subject to little or no influence from ozone and water vapor absorption, these terms will be neglected. Molecular Rayleigh scattering and absorption can be calculated for each band. The remainder of the total optical depth is assumed to be due to aerosol content. As this technique will mainly be applied in areas where other techniques fail, certain assumptions about the nature of the observed aerosols, such as source regions and likely size distributions, will be possible. This will aid in the proper characterization of the aerosol optical depth. Fig. 2 provides a schematic of the radiation paths illuminating the surface.

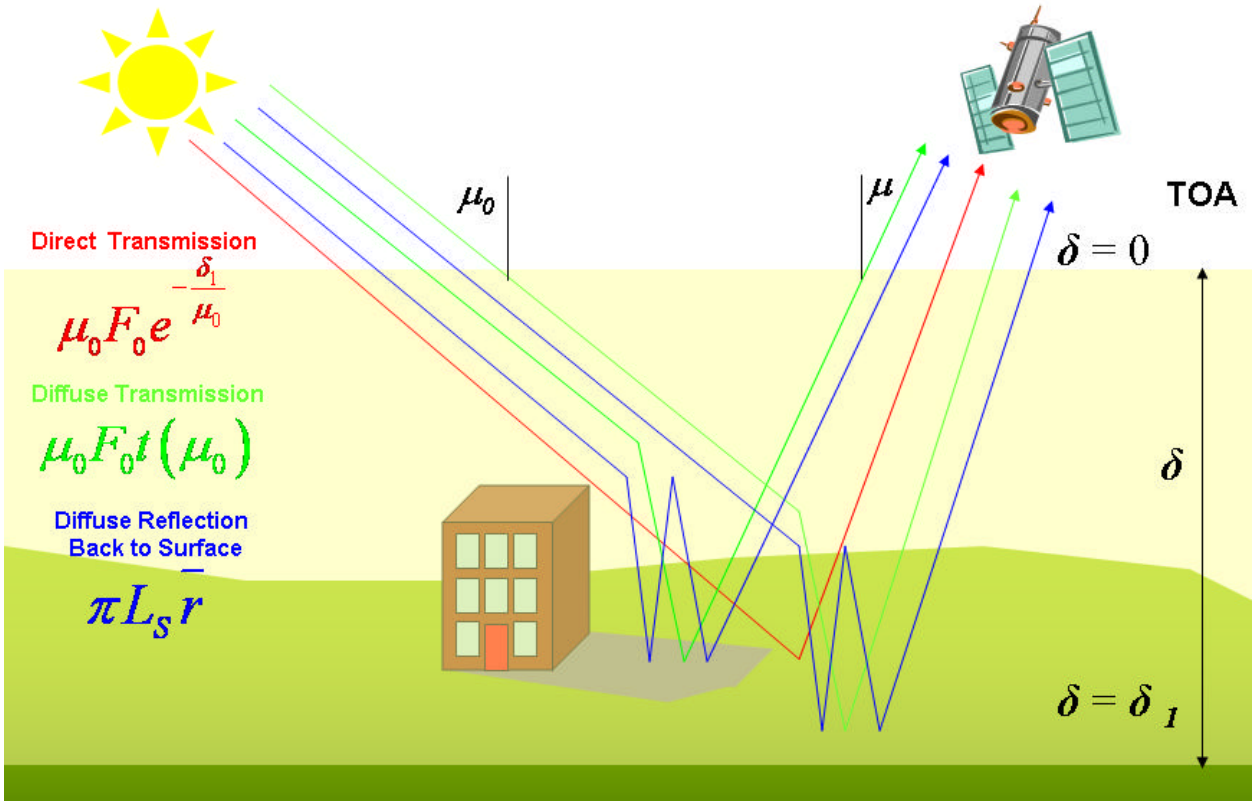

Figure 2. The shadow method uses the difference between the radiances within and outside of the shadowed area to quantify the direct transmission and the total optical depth.

A more rigorous development of the governing equation begins with a simple flux density, or irradiance, balance between the upward and downward flux density. When surface reflectance due to a Lambertian surface is considered, this becomes:

$$pL_s = r_s \times \textit{downward flux density},$$

where r_s is surface reflectance and L_s is the upward surface radiance. The downward flux density can be partitioned into three components depicted in Fig. 2; direct transmission, diffuse transmission, and the component of surface radiance reflected by the atmosphere.

Now, the flux density balance may be described using the terms depicted in Fig. 2 as

$$p\,L_s = r_s\left(m_0 F_0 e^{-d_1/m_0} + m_0 F_0 t(m_0) + p\,L_s \bar{r}\right), \quad (1)$$

where m_0 is the cosine of the solar zenith angle, F_0 is the incoming solar irradiance at the TOA, d_1 is the total aerosol optical depth, $t(m_0)$ is the diffuse transmittance term, and $\bar{r}$ is the mean aerosol reflectance. Eq. (1) can be solved for L_s, surface intensity or radiance,

$$L_s = \frac{r_s}{1 - r_s \bar{r}} \frac{m_0 F_0}{p}\left(e^{-d_1/m_0} + t(m_0)\right). \quad (2)$$

Eq. (2) represents the radiance as measured at the surface. When viewed from the satellite, the directly transmitted surface leaving radiance is again subject to attenuation as measured by the optical depth of the atmosphere. As such, Eq. (2) then becomes:

$$L_s = \left[\frac{r_s}{1 - r_s \bar{r}} \frac{m_0 F_0}{p}\left(e^{-d_1/m_0} + t(m_0)\right)\right] e^{(-d_1/m)}, \quad (3)$$

where the additional extinction term is a function of μ, the cosine of the viewing zenith angle, representing the path loss due to the optical depth from the surface to the satellite sensor.

Eq. (3) provides a convenient way to quickly determine all factors affecting the observed surface radiance. Applying this equation to the original problem of characterizing aerosol optical depth from high-spatial resolution imagery, we can use Eq. (3) unaltered to represent that radiance we would observe outside of shaded areas within the image.

A slight adjustment to Eq. (3) must be made when we consider shaded areas. By definition, a shaded region lacks the direct transmission term described in Fig. 2. Removing this term, but retaining the contributions due to diffuse transmission and atmosphere reflected surface radiance, one gets

$$L_s^{shaded} = \left[\frac{r_s}{1 - r_s \bar{r}} \frac{m_0 F_0}{p} t(m_0) \right] e^{(-d_1/m)}. \quad (4)$$

At the high spatial resolutions found in QuickBird imagery, one can easily observe surface radiance both within and outside of shaded areas. If an area adjacent, but just outside of the shaded area is chosen such that the surface reflectance of the shaded and unshaded areas is the same, then we can take the difference between Eqs. (3) and (4) to characterize the observed difference in intensities

$$L_s^{unshaded} - L_s^{shaded} = L_d = \frac{r_s}{1 - r_s \bar{r}} \frac{m_0 F_0}{p} e^{-d_1 \left(\frac{1}{m_0} + \frac{1}{m} \right)}. \quad (5)$$

Solving Eq. (5) for total optical depth, d_1, the governing equation for optical depth retrieval from satellite-measured radiances becomes:

$$d_1 = \left(\frac{m_0 m}{m + m_0} \right) \ln \left[\left(\frac{r_s}{1 - r_s \bar{r}} \right) \left(\frac{m_0 F_0}{p L_d} \right) \right]. \quad (6)$$

Eq. (6) now becomes the governing equation for retrieving total optical depth from the difference in satellite measured radiances using a known solar irradiance specific to the channel considered and viewing and solar geometries.

An iterative approach must be used when retrieving total optical depth with Eq. (6) since no *a priori* knowledge of surface reflectance or mean aerosol reflectance is available. In the first iteration, mean aerosol reflectance is assumed to be much smaller than surface reflectance such that the product of surface reflectance and mean aerosol reflectance is much less than one. Additionally, the top of the atmosphere (TOA) reflectance for the unshaded region is used as the surface reflectance for the first iteration. Sensitivity and uncertainty analyses indicate that uncertainty in surface reflectance is of the second order as compared to the difference in observed radiances and that retrievals are quite stable for surface reflectance above 0.05. An approximate total optical depth is retrieved and subsequently used to determine a mean aerosol reflectance. This mean aerosol reflectance is subtracted from the surface (TOA) reflectance determined from the unshaded region, and total optical depth is again retrieved using Eq. (6) in its entirety. This retrieved total optical depth is then corrected for molecular Rayleigh scattering to produce an aerosol optical depth.

3. APPLICATION AND METHODS

QuickBird panchromatic imagery was chosen for this investigation due to its ability to easily resolve shadows of typical urban scale structures such as buildings. QuickBird panchromatic imagery covers the spectrum from 445 to 900 nanometers with an effective central wavelength of 673 nanometers. A program was constructed to carry out the initial retrieval using TOA reflectance as the surface reflectance. Then, using the initially retrieved optical depth, the mean aerosol reflectance was determined. The mean aerosol reflectance is then used to adjust the TOA reflectance to better represent surface reflectance. A second total optical depth retrieval is carried out with these new values and the retrieved optical depth was corrected for molecular Rayleigh scattering.

A QuickBird panchromatic image of the Mobile Atmospheric Aerosol and Radiation Characterization Observatory (MAARCO) site northeast of Abu Dhabi on September 16th, 2004 during the Unified Aerosol Experiment – United Arab Emirates (UAE^2) was used to test the Shadow technique for AOD retrieval. Aerosol optical depth was retrieved for 18 sites across the single 16.5 kilometers by 16.5 kilometers image from modal radiances (both within and outside of the shadowed area) using the technique described above. The mean aerosol reflectance calculation is based on the Henyey-Greenstein phase function and requires a single scatter albedo and an asymmetry parameter. In this case, a single scatter albedo of 0.94 and an asymmetry parameter of 0.65

were used (Reid 2005). The results as compared to the AERONET Level 2.0 AOD retrieval taken six minutes prior to the image are shown in Fig. 3. The QuickBird panchromatic sensor response curves were used to integrate over the narrowband AERONET AOD retrievals between 440 and 870 nanometers to determine an integrated AOD at the effective center wavelength of the panchromatic band, 673 nanometers.

4. RESULTS

Eighteen aerosol optical depth retrievals were accomplished across a variety of backgrounds within the QuickBird panchromatic image using the Shadow technique. Retrieved aerosol optical depths ranged from 0.14 to 0.34 with a mean of 0.20 and a standard deviation of 0.05. This compares reasonably well to the integrated AERONET aerosol optical depth retrieval centered at 673.1 nanometers of 0.23. A histogram of the 18 cases is shown in Fig. 3. Nine of the cases fell between 0.18 and 0.24 and 16 cases fell between 0.14 and 0.24 showing a high level of consistency in the retrievals. Additionally, the retrieved surface reflectances ranged from 0.14 to 0.30 and compared well to the expected values for the backgrounds used. Of the 18 cases, nine had surface reflectances of less than 0.2 and typically came from backgrounds of dark or weathered pavement. These results show that retrieved AODs are realistic and consistent, as are surface reflectances derived from the image.

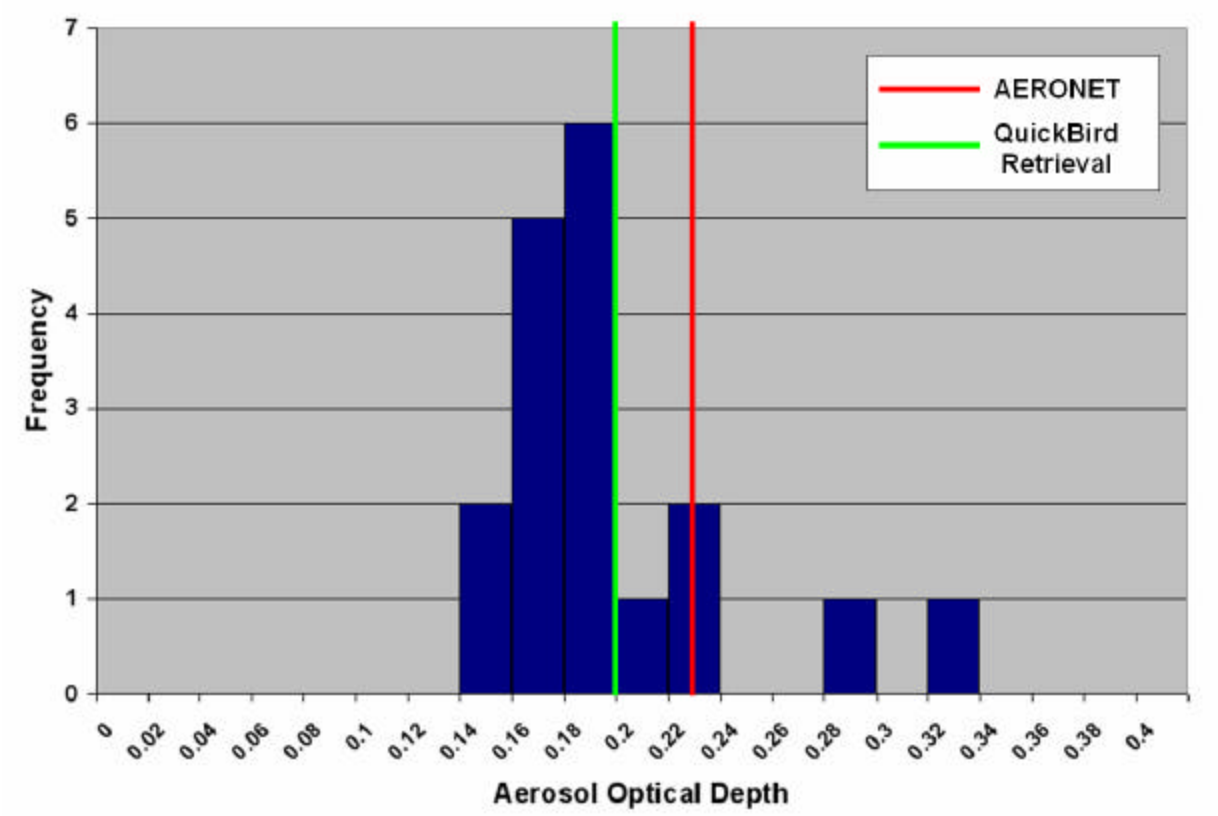

Figure 3. Histogram of AOD retrievals from 18 sites in the September 16, 2004 QuickBird image of the MAARCO site northeast of Abu Dhabi, UAE during the UAE^2 campaign with the AERONET AOD retrieval in red and the mean of the QuickBird AOD retrievals in green.

5. CONCLUSION

A new method of aerosol optical depth retrieval is proposed in this paper based on shadows observed in high spatial resolution commercial satellite imagery. Unlike previous contrast reduction techniques for AOD retrieval, this technique is physically based and does not require a training data set. Assumptions include a Lambertian surface and aerosol physical properties described solely by a single scatter albedo and asymmetry parameter. Uncertainty analysis indicates that aerosol optical depth retrievals should be possible within ±0.04. Initial results are

encouraging and indicate that the average of many retrievals over a typical high-resolution commercial satellite scene can provide a reliable estimate of aerosol optical depth within the scene.

Acknowlegments

The authors would like to thank Brent Holben and his staff for the maintaining and processing the AERONET site and data used in this study. We would also like to thank the Office of his Highness the President – Department of Water Resource Studies (DWRS) – United Arab Emirates for their support of the UAE^2 campaign.

REFERENCES

Abdou, W. A., D. J. Diner, J. V. Martonchik, C. J. Bruegge, R. A. Kahn, B. J. Gaitley, and K. A. Crean, 2005: Comparison of coincident Multiangle Imaging Spectroradiometer and Moderate Resolution Imaging Spectroradiometer aerosol optical depths over land and ocean scenes containing Aerosol Robotic Network sites. *J. Geophys. Res.*, **110**, D10S07, doi:10.1029/2004JD004693.

Ambartzumian, V. A., 1958: *Theoretical Astrophysics*. Pergamon, 645 pp.

Brown, B. B., 1997: Remote measurement of aerosol optical properties using NOAA POES AVHRR and GOES Imagery during TARFOX. M. S. Thesis, Department of Meteorology, Naval Postgraduate School, CA, 73 pp.

Charlson, R. J., S. E. Swartz, J. M. Hales, R. D. Cess, J. A. Coakley, Jr., J. E. Hansen and D. J. Hoffman, 1992: Climate forcing by anthropogenic aerosols. *Science*, **255**, 423-430.

DigitalGlobe, cited 2005: QuickBird technical specifications. [Available online at http://www.digitalglobe.com/about/quickbird.html.]

Durkee, P. A., K. E. Nielsen, P. J. Smith, P. B. Russell, B. Schmid, J. M. Livingston, B. N. Holben, C. Tomasi, V. Vitale, D. Collins, R. C. Flagan, J. H. Seinfeld, K. J. Noone, E. Ostrom, S. Gasso, D. Hegg, L. M. Russell, T. S. Bates, and P. K. Quinn, 2000: Region aerosol optical depth characteristics from satellite observations: ACE-1, TARFOX, and ACE-2 results. *Tellus,* **52(B)**, 484-497.

Hsu, N. C., S. C. Tsay, M. D. King, and J. R. Herman, 2004: Aerosol properties over bright-reflecting source regions. *IEEE Trans. Geosci. Remote Sensing*, **42**, 557-569.

Intergovernmental Panel on Climate Change. *Climate Change 2001 – The Scientific Basis* (contribution of working group I to the Third Assessment Report of the Intergovernmental Panel on Climate Change). Cambridge University Press, Cambridge, 2001.

Kahn, R. A., B. J. Gaitley, J. V. Martonchik, D. J. Diner, and K. A. Crean, 2005: Multiangle Imaging Spectroradiometer (MISR) global aerosol optical depth validation based on 2 years of coincident Aerosol Robotic Network (AERONET) observations. *J. Geophys. Res.*, **110**, D10S04, doi:10.1029/2004JD004706.

Kaufman, Y. J., and R. S. Fraser, 1984: Atmospheric effect on classification of finite fields. *Rem. Sens. Env.*, **15**, 95-118.

Kaufman, Y. J., and J. H. Joseph, 1982: Determination of surface albedos and aerosol extinction characteristics from satellite imagery. *J. Geophys. Res.*, **87**, 1287-1299.

Kaufman, Y. J., and C. Sendra, 1988: Algorithm for automatic atmospheric corrections to visible and near-IR satellite imagery. *Int. J. Remote Sens.*, **9**, 1357-1381.

Kiehl, J. T., and B. P. Briegleb, 1993: The relative roles of sulfate aerosols and greenhouse gases in climate forcing. *Science*, **260**, 311-314.

Kuciauskas, A. P., 2002: Aerosol optical depth analysis with NOAA GOES and POES in the Western Atlantic. M. S. thesis, Dept. of Meteorology, Naval Postgraduate School, Monterey, CA, 101 pp.

Liou, K. N., 2002: *An Introduction to Atmospheric Radiation*. Academic Press, pp. 583.

Martin, J. S., 2004: Aerosol optical depth model assessment with high resolution multiple angle sensors. M. S. thesis, Dept. of Meteorology,

Naval Postgraduate School, Monterey, CA, 53 pp.

Odell, A. P., and J. A. Weinman, 1975: The effect of atmospheric haze on images of the earth's surface. *J. Geophys. Res.*, **80**, 5035-5040.

Prather, M. J., 1996: Time scales in atmospheric chemistry: Theory, GWPs for CH4 and CO, and runaway growth. *Geophys. Res. Lett.*, **23**, 2597-2600.

Reid, J. S., 2005: Personal Communication.

Remer, L. A., Y. J. Kaufman, D. Tanre, S. Mattoo, D. A. Chu, J. V. Martins, R.-R. Li, C. Ichoku, R. C. Levy, R. G. Kleidman, T. F. Eck, E. Vermote, and B. N. Holben, 2005: The MODIS aerosol algorithm, products, and validation. *J. Atmos. Sci.*, **62**, 947-973.

Smith, S. J., and T. M. L. Wigley, 2000: Global warming potentials: 1. Climatic implications of emissions reductions. *Climatic Change*, **44**, 445-457.

Tanre, D., M. Herman, and P. Y. Deschamps, 1981: Influence of the background contribution upon space measurements of ground reflectance. *Appl. Opt.*, **20**, 3676-3684.

Tanre, D., P. Y. Deschamps, C. Devaux, and M. Herman, 1988: Estimation of Saharan aerosol optical thickness from blurring effects in Thematic Mapper data. *J. Geophys. Res.*, **93**, 15955-15964.

Tanre, D., and M. Legrand, 1991: On the satellite retrieval of Saharan dust optical thickness over land: Two different approaches. *J. Geophys. Res.*, **96**, 5221-5227.

Twomey, S. A., M. Piepgrass, and T. L. Wolfe, 1984: An assessment of the impact of pollution on the global albedo. *Tellus,* **36(B)**, 356-366.